ORIGINAL PAPER

In vivo comparison of arterial lumen dimensions assessed by co-registered three-dimensional (3D) quantitative coronary angiography, intravascular ultrasound and optical coherence tomography

**Shengxian Tu · Liang Xu · Jurgen Ligthart · Bo Xu ·
Karen Witberg · Zhongwei Sun · Gerhard Koning ·
Johan H. C. Reiber · Evelyn Regar**

Abstract This study sought to compare lumen dimensions as assessed by 3D quantitative coronary angiography (QCA) and by intravascular ultrasound (IVUS) or optical coherence tomography (OCT), and to assess the association of the discrepancy with vessel curvature. Coronary lumen dimensions often show discrepancies when assessed by X-ray angiography and by IVUS or OCT. One source of error concerns a possible mismatch in the selection of corresponding regions for the comparison. Therefore, we developed a novel, real-time co-registration approach to guarantee the point-to-point correspondence between the X-ray, IVUS and OCT images. A total of 74 patients with indication for cardiac catheterization were retrospectively included. Lumen morphometry was performed by 3D QCA and IVUS or OCT. For quantitative analysis, a novel, dedicated approach for co-registration and lumen detection was employed allowing for assessment of lumen size at multiple positions along the vessel. Vessel curvature was automatically calculated from the 3D arterial vessel centerline. Comparison of 3D QCA and IVUS was performed in 519 distinct positions in 40 vessels. Correlations were $r = 0.761$, $r = 0.790$, and $r = 0.799$ for short diameter (SD), long diameter (LD), and area, respectively. Lumen sizes were larger by IVUS ($P < 0.001$): SD, 2.51 ± 0.58 mm versus 2.34 ± 0.56 mm; LD, 3.02 ± 0.62 mm versus 2.63 ± 0.58 mm; Area, 6.29 ± 2.77 mm^2 versus 5.08 ± 2.34 mm^2. Comparison of 3D QCA and OCT was performed in 541 distinct positions in 40 vessels. Correlations were $r = 0.880$, $r = 0.881$, and $r = 0.897$ for SD, LD, and area, respectively. Lumen sizes were larger by OCT ($P < 0.001$): SD, 2.70 ± 0.65 mm versus 2.57 ± 0.61 mm; LD, 3.11 ± 0.72 mm versus 2.80 ± 0.62 mm; Area 7.01 ± 3.28 mm^2 versus 5.93 ± 2.66 mm^2. The vessel-based discrepancy between 3D QCA and IVUS or OCT long diameters increased with increasing vessel curvature. In conclusion, our comparison of co-registered 3D QCA and invasive imaging data suggests a bias towards larger lumen dimensions by IVUS and by OCT, which was more pronounced in larger and tortuous vessels.

S. Tu (✉) · G. Koning · J. H. C. Reiber
Division of Image Processing, Department of Radiology, Leiden University Medical Center, Albinusdreef 2, 2300 RC Leiden, The Netherlands
e-mail: S.T.Tu@lumc.nl

L. Xu · B. Xu (✉) · Z. Sun
Catheterization Lab, National Center for Cardiovascular Diseases of China and Fu Wai Hospital, A 167, Beilishi Road, Xicheng District Beijing, Beijing 100037, China
e-mail: bxu@citmd.com

J. Ligthart · K. Witberg · E. Regar
Department of Cardiology, ErasmusMC, Rotterdam, The Netherlands

🖄 Springer

Abbreviations

DICOM	Digital imaging and communications in medicine
ED	End-diastolic
IVUS	Intravascular ultrasound
LAD	Left anterior descending
LAO	Left anterior oblique
LCx	Left Circumflex Artery
LD	Long diameter
OCT	Optical coherence tomography
OM	Obtuse Marginal
QCA	Quantitative coronary angiography
RCA	Right coronary artery
RAO	Right anterior oblique
RI	Ramus Intermedius
SD	Short diameter

Introduction

Coronary lumen dimensions often show discrepancies when assessed by X-ray angiography and invasive imaging such as intravascular ultrasound (IVUS) or optical coherence tomography (OCT) [1]. One source of error consists of a possible mismatch in the selection of corresponding regions for the comparison of different imaging modalities. Therefore, we developed a novel, real-time co-registration approach to guarantee the point-to-point correspondence between the X-ray, IVUS and OCT images. This study compared lumen size as assessed in vivo by co-registered three-dimensional quantitative coronary angiography (3D QCA) and IVUS or OCT in both frame-based and vessel-based approaches. In addition, we hypothesized that the vessel-based discrepancy between 3D QCA and IVUS or OCT was associated with vessel curvature, a surrogate for vessel tortuosity, since tortuous vessels might change the alignment of the intracoronary imaging catheter inside the lumen, resulting in inaccurate lumen dimensions when the catheter was positioned obliquely (not parallel to the vessel long-axis direction). Therefore, vessel curvature was also assessed in this study and its association with the discrepancy between 3D QCA and IVUS/OCT was assessed. The looseness of the catheter, i.e., the space between the lumen-intima interface and the imaging catheter was used as a confounder to analyze

the aforementioned association. The more space between the catheter and the lumen-intima interface, the more oblique the catheter could be positioned in tortuous vessels, possibly leading to more overestimation of lumen size by IVUS/OCT at certain regions. As a result, the discrepancy between 3D QCA and IVUS/OCT might increase. On the other hand, less catheter looseness creates less chance of oblique imaging. A catheter looseness of zero indicates that the imaging catheter fits tightly in the vessel. In such a case, IVUS/OCT images represent at every location the cross-section perpendicular to the vessel long-axis direction. The impact of vessel curvature on the discrepancy between 3D QCA and IVUS/OCT is then minimal or actually absent.

Methods

Study population

At the Catheterization Lab, National Center for Cardiovascular Diseases of China and Fu Wai Hospital in Beijing, China, and the Department of Cardiology, ErasmusMC in Rotterdam, the Netherlands, a total of 74 patients with indication for cardiac catheterization were retrospectively included in this study. Inclusion criteria were: (1) X-ray angiographic images were acquired by digital image intensifiers (flat-panel systems). (2) Two angiographic projections at least 25° apart with lumen well filled with contrast dye agent were recorded. (3) The vessel of interest was imaged with motorized IVUS or OCT pullbacks at constant pullback speeds. (4) The vessel of interest was not totally occluded and had no history of coronary bypass surgery. (5) If stents were present in the vessel of interest, the entire IVUS/OCT pullback series completely imaged another non-stented lesion.

Angiographic images were recorded by different X-ray systems (AXIOM-Artis, Siemens, Erlangen, Germany; AlluraXper, Philips, Best, the Netherlands; and Safair, Shimadzu, Kyoto, Japan). The angiographic images used for 3D QCA were acquired prior to inserting the guidewire and intracoronary imaging catheter. Grayscale IVUS imaging was carried out using a 40 MHz transducer and a 2.9 F imaging sheath with a dedicated workstation (Atlantis SR Pro and Galaxy, Boston Scientific, Boston, MA, USA). Images were recorded at 30 frames/s and converted to DICOM

(Digital imaging and communications in medicine) format at a resolution of 512 × 512 pixels. OCT pullbacks were performed at 20 mm/s by non-occlusive flushing technique using a 2.7 F imaging catheter with a dedicated workstation (C7 Dragonfly and C7-XR, Lightlab Imaging, Westford, MA, USA). OCT images were recorded at 100 frames/s and converted to DICOM format at a resolution of 512 × 512 pixels. Z-offset calibration was performed before converting to DICOM format for the subsequent analysis.

Three-dimensional quantitative coronary angiography

3D angiographic reconstruction and quantitative analysis were performed by an experienced analyst using a novel and validated 3D QCA software package (prototype version, Medis medical imaging systems bv, Leiden, the Netherlands) [2–4]. The following steps were used as standard operation procedures in the study: (1) two image sequences acquired at two arbitrary angiographic views with projection angles at least 25° apart were loaded; (2) automated calibration or manual catheter calibration if the so-called Pixel Spacing parameter was not recorded by the X-ray systems was performed; (3) properly contrast-filled end-diastolic (ED) frames of these angiographic image sequences were selected; (4) one to three anatomical markers, e.g., bifurcations, were identified as reference points in the two angiographic views for the automated correction of angiographic system distortions [5]; (5) the vessel segment of interest was defined and automated 2D lumen edge detection was performed using our extensively validated QCA algorithms [6, 7]; (6) automated 3D reconstruction and modeling techniques were performed. The resulting lumen surface modeled with elliptical cross-sections and the so-called reference surface modeled with circular cross-sections were generated. Quantitative data including the global parameters, e.g., lumen volume, diameter and area stenoses, and the local parameters at every position along the vessel segment of interest, e.g., short diameter, long diameter, and area were automatically reported.

An example of 3D angiographic reconstruction of the Left Circumflex Artery (LCx) is given in Fig. 1. The two angiographic views acquired at 56 LAO, 19 Caudal and 13 RAO, 23 Caudal were used for the 3D reconstruction. The left top panels (Fig. 1a, b) show the segment of interest in the LCx and its extracted 2D contours, superimposed on the two angiographic views. The left bottom panel (Fig. 1c) shows the 3D reconstructed lumen surface in a color-coded fashion. In this case, the lesion at the proximal LCx had a minimum lumen diameter of 1.11 mm. The diameter and area stenoses were found to be 68.1 and 82.7%, respectively.
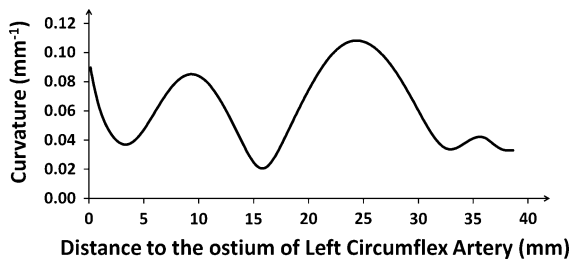
Calculation of vessel curvature

Intuitively, vessel curvature is the amount by which the vessel deviates from being a straight tube. Tortuous or bended vessels have higher curvature than straight vessels. At every position along the tortuous vessel, there is a unique circle which best approximates the vessel segment. The radius of that circle is equal to the reciprocal of the curvature. To determine the curvature at each position along the vessel of interest, the reconstructed arterial centerline was approximated by a parameterized Bezier curve, which is frequently used in modeling smooth curves/surfaces in computer graphics and related fields. In such a way the derivatives of the vessel were estimated by the Bezier curve and the curvature was calculated using the first and second derivatives. Figure 2 shows the curvature profile for the LCx segment reconstructed in Fig. 1. The carina position of the LCx/OM (Obtuse Marginal) bifurcation has the highest curvature of 0.1082 mm^{-1}. The vessel curvature was defined as the average curvature for all the positions along the vessel of interest. In this case, the vessel curvature is 0.0615 mm^{-1} for the reconstructed segment.

Registration of 3D QCA with IVUS or OCT

Over the past years we have developed and validated a real-time and straightforward approach for the on-line registration of 3D QCA with IVUS/OCT [8]. The approach only requires the operator to reconstruct the arterial centerline from two angiographic images (which is a standard module in 3D QCA software packages). The step of reconstructing the IVUS/OCT pullback trajectory as required by conventional approaches was replaced by a novel distance mapping algorithm which estimated the corresponding IVUS/OCT cross-sectional image for each position along the reconstructed arterial centerline, based on the accumulated curvature and
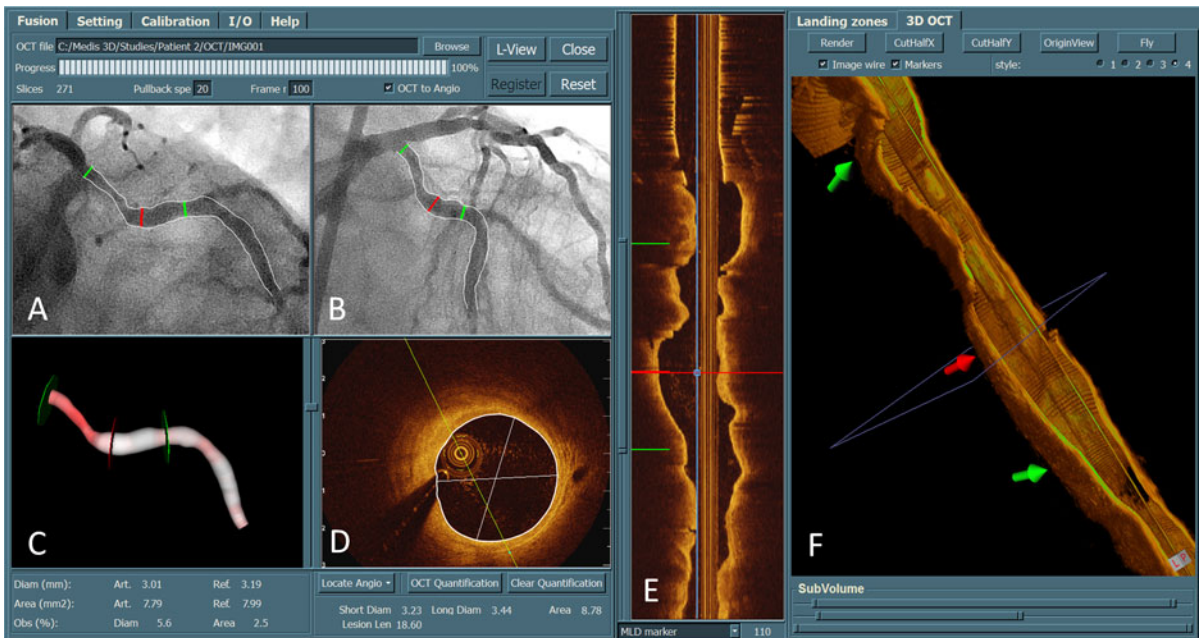
Fig. 1 Three-dimensional coronary angiographic reconstruction and its registration with 3D OCT. After the registration, the corresponding markers in different views (**a**, **b**, **c**, **e**, and **f**) were synchronized, allowing the assessment of lumen dimensions from both imaging modalities at every corresponding position along the vessel segment

Fig. 2 The curvature profile assessed from the 3D reconstructed Left Circumflex Artery. The average curvature is 0.0615 mm^{-1} for the reconstructed segment

lumen size as assessed from 3D QCA. By this approach, the disadvantage of using diluted contrast agent during angiographic image acquisitions, as required by conventional registration approaches [9, 10] in order to simultaneously visualize the lumen and the imaging catheter, was resolved and as a result, the quality of 3D QCA was improved and less manual corrections were required in the lumen edge detection. Minimum user interactions were achieved in this registration approach by indicating only one anatomical or mechanical landmark that was visualized in both X-ray and IVUS/OCT images, e.g., the carina of a bifurcation. After the registration, point-to-point correspondence between the X-ray and IVUS/OCT images was established and markers superimposed on different image views were synchronized. Figure 1 shows three positions with corresponding markers superimposed in the 2D and 3D angiographic views (a, b, and c) as well as the 3D OCT and longitudinal views (f and e).

The registration for all the vessels was performed by an experienced analyst and the results were verified by an expert in intracoronary imaging using landmarks available along the vessel of interest. In such a way the reliability of the registration was guaranteed.

Frame selection and quantitative IVUS/OCT analysis

A number of spatial positions including normal and obstructed cross-sections along the vessel of interest were selected for the quantitative analysis. A constant stepping interval depending on the length of the vessel of interest was initially applied in the selection procedure to guarantee that a couple of positions (at least 8) were selected for each vessel. If thrombosis, plaque erosion or dissection was identified in the selected frames, or if the corresponding vessel positions in the angiographic images had severe overlap

that could jeopardize the reliability of the lumen contour delineation in QCA, the adjacent frames were selected. If predilation or thrombectomy was performed before intracoronary imaging, the injured subsegments were excluded. Bifurcations were excluded as well since there was no well-established standard to compare bifurcation dimensions between 3D QCA and IVUS or OCT. In such a way a couple of reliably co-registered positions were analyzed for each vessel and the variability introduced by the analysis methodology itself was reduced. As a result, the comparisons reflected the systematic difference between 3D QCA and IVUS or OCT. For IVUS images, only frames that corresponded to the ED phase in the cardiac cycle were considered, since 3D QCA was performed also at the ED phase. A well validated algorithm integrated in a commercial software package (QIvus 2.1, Medis medical imaging systems bv, Leiden, the Netherlands) [11] was used for the IVUS segmentation and quantitative analysis. For quantitative OCT analysis, a new mincost algorithm was directly integrated in the registration software to automatically detect the lumen-intima interface from OCT images. The algorithm used the asymmetric sticks [12] to construct a matrix with each cell representing the edge strength/probability for the corresponding position. In a next step, a global optimization algorithm, the so-called mincost algorithm, was applied to find the optimal path (lumen-intima interface) with the strongest edge strength. An example of comparing lumen dimensions as assessed from 3D QCA and OCT is given by Fig. 1. In this case, short diameter, long diameter, and lumen area at the position indicated by the middle (red) marker were 3.23, 3.44 mm, and 8.78 mm^2 by OCT, as compared with 3.01 mm, 3.30, and 7.79 mm^2 by 3D QCA.

Frame-based comparison between 3D QCA and IVUS or OCT was performed on all the selected positions. The mean lumen size calculated from all the selected positions for each vessel was used to represent the lumen size for that specific vessel and used for the vessel-based comparison. To assess the association of the discrepancy between 3D QCA and IVUS or OCT with vessel curvature, the confounder, i.e., the looseness of the IVUS/OCT imaging catheter, was derived, defined by the long lumen diameter minus the catheter diameter. Accordingly, larger lumen diameter yielded larger catheter looseness. Since lumen diameters were unknown in this study, the average value of

the 3D QCA and IVUS/OCT long diameters was used to calculate the catheter looseness.

Quantitative IVUS/OCT analysis was performed on the selected corresponding positions by an analyst, who was unaware of the 3D QCA results. The measurements in the first 10 vessels were repeated by the same analyst 1 month later, and by a second analyst, both blinded to the earlier results. From these measurements, intra- and inter-observer variabilities were derived.

Statistics

3D QCA was compared with IVUS or OCT by using paired t-test, while the differences were evaluated by Bland–Altman plots. Quantitative data were presented as mean difference $\pm$ standard deviation and the correlations were assessed by using Pearson's correlation coefficient, providing the correlation coefficient (R) and the regression line. A 2-sided P-value of <0.05 was considered to be significant. Confounders independently influencing the vessel-based discrepancy between 3D QCA and IVUS or OCT were analyzed using a stepwise multiple linear regression. The intra- and interobserver variabilities were reported as mean difference $\pm$ standard deviation. All statistical analyses were carried out using SPSS software (PASW version 18.0.0, 2009; SPSS Inc, Chicago, IL).

Results

The baseline characteristics for the included patients and assessed vessels are given in Table 1. A total of 40 vessels (LAD = 35, LCx = 5, Diagonal = 1, RCA = 1) from 37 patients were included to compare lumen size by 3D QCA and by IVUS. In 4 of these vessels, manual calibration had to be performed in the 3D angiographic reconstruction. For the remaining 36 vessels, automated calibration was applied. The segment of interest had a mean diameter stenosis of 45.5% as assessed from 3D QCA. 24 vessels were revascularized after the examinations. A total of 40 vessels (LAD = 22, LCx = 5, OM = 1, RCA = 11, Ramus Intermedius = 1) from the other 37 patients were included to compare 3D QCA and OCT. Automated calibration was applied for all the vessels in the 3D angiographic reconstruction. The assessed segments of interest had a mean diameter stenosis of

45.4% as assessed from 3D QCA. 25 vessels were revascularized after the examinations.

A total of 519 distinct positions were selected for the comparison between 3D QCA and IVUS in measuring short diameter (SD), long diameter (LD) and lumen area. Scatter plots of the comparison are presented in Fig. 3. There were good correlations between 3D QCA and IVUS: SD ($r = 0.761$, $P < 0.001$); LD ($r = 0.790$, $P < 0.001$); Area ($r = 0.799$, $P < 0.001$). Bland–Altman plots in Fig. 3b′ and c′ show that there was an increasing bias towards larger lumen size by IVUS, which was more pronounced in larger vessels. Quantitative data are presented in Table 2. Lumen sizes were larger by IVUS than by 3D QCA: SD 2.51 ± 0.58 mm versus 2.34 ± 0.56 mm ($P < 0.001$); LD 3.02 ± 0.62 mm versus 2.63 ± 0.58 mm ($P < 0.001$); Area 6.29 ± 2.77 mm^2 versus 5.08 ± 2.34 mm^2 ($P < 0.001$) in frame-based analysis. The difference was 0.16 mm (6.6%) in SD, 0.39 mm (13.8%) in LD, and 1.21 mm^2 (21.3%) in area. Vessel-based analysis showed similar discrepancies: SD 2.53 ± 0.39 mm versus 2.35 ± 0.37 mm ($P < 0.001$); LD 3.05 ± 0.43 mm versus 2.64 ± 0.36 mm ($P < 0.001$); Area 6.41 ± 1.92 mm^2 versus 5.12 ± 1.45 mm^2 ($P < 0.001$).

A total of 541 distinct positions were selected for the comparison between 3D QCA and OCT. Scatter plots of the comparison are presented in Fig. 4. Good correlations were found between 3D QCA and OCT: SD ($r = 0.880$, $P < 0.001$); LD ($r = 0.881$, $P < 0.001$); Area ($r = 0.897$, $P < 0.001$). Bland–Altman plots in Figs. 4b′ and c′ show that there was an increasing bias towards larger lumen size by OCT, which was more pronounced in larger vessels. Quantitative data are presented in Table 3. Lumen sizes were larger by OCT than by 3D QCA: SD 2.70 ± 0.65 mm versus 2.57 ± 0.61 mm ($P < 0.001$); LD 3.11 ± 0.72 mm versus 2.80 ± 0.62 mm ($P < 0.001$); Area 7.01 ± 3.28 mm^2 versus 5.93 ± 2.66 mm^2 ($P < 0.001$) in frame-based analysis. The difference was 0.14 mm (5.3%) in SD, 0.30 mm (10.2%) in LD, and 1.07 mm^2 (16.5%) in area. Vessel-based analysis showed similar discrepancy: SD 2.71 ± 0.46 mm versus 2.57 ± 0.43 mm ($P < 0.001$); LD 3.11 ± 0.52 mm versus 2.81 ± 0.45 mm ($P < 0.001$); Area 7.02 ± 2.34 mm^2 versus 5.94 ± 1.91 mm^2 ($P < 0.001$).

Figure 5 shows the vessel-based discrepancy between 3D QCA and IVUS/OCT with respect to the vessel curvature. There was a bias towards larger discrepancy in vessels with higher curvature, which was more pronounced for long diameter. The independent association of the discrepancy between 3D QCA and IVUS/OCT with vessel curvature and catheter looseness is given by Table 4. The discrepancy in long diameters as assessed by 3D QCA and by IVUS was associated with vessel curvature ($P = 0.02$) and catheter looseness ($P = 0.02$). Linear regression equation was: (IVUS - 3D QCA) Long Diameter $= 5.323 \times$ Vessel Curvature $+ 0.204 \times$ Catheter Looseness $- 0.072$. Similarly, the discrepancy in long diameters as assessed by 3D QCA and by OCT was associated with vessel curvature ($P = 0.02$) and catheter looseness ($P = 0.04$). Linear regression equation was: (OCT - 3D QCA) Long Diameter $= 4.627 \times$ Vessel Curvature $+ 0.137 \times$ Catheter Looseness $- 0.147$.

Table 1 Baseline characteristics

	IVUS	OCT
Patient	$n = 37$	$n = 37$
Age	55.8 (41–75)	60 (44–78)
Male/female	26/11	21/16
Imaged vessel	$n = 40$	$n = 40$
LAD/Diagonal/LCx/OM/RCA/RI	35/1/5/1/0/0	22/0/5/1/11/1
Stents in subsegment	19	1
Assessed lesion		
Predilatated before intracoronary imaging	6	3
Ostial or bifurcation lesion	23	13
Diffused lesion	18	11
Calcified lesion	13	23
Diameter stenosis[a]	45.5(±12.5)%	45.4(±17.0)%
Lesion treated later by revascularization	24	25

[a] Assessments based on 3D QCA

LAD Left anterior descending, *LCx* Left Circumflex Artery, *OM* obtuse marginal, *RCA* right coronary artery, *RI* Ramus Intermedius

Discussions

Over the past years, the continuous development in coronary quantitative analysis has been motivated by the increasing need to better assess the true dimensions of vascular structures and by the on-line support of
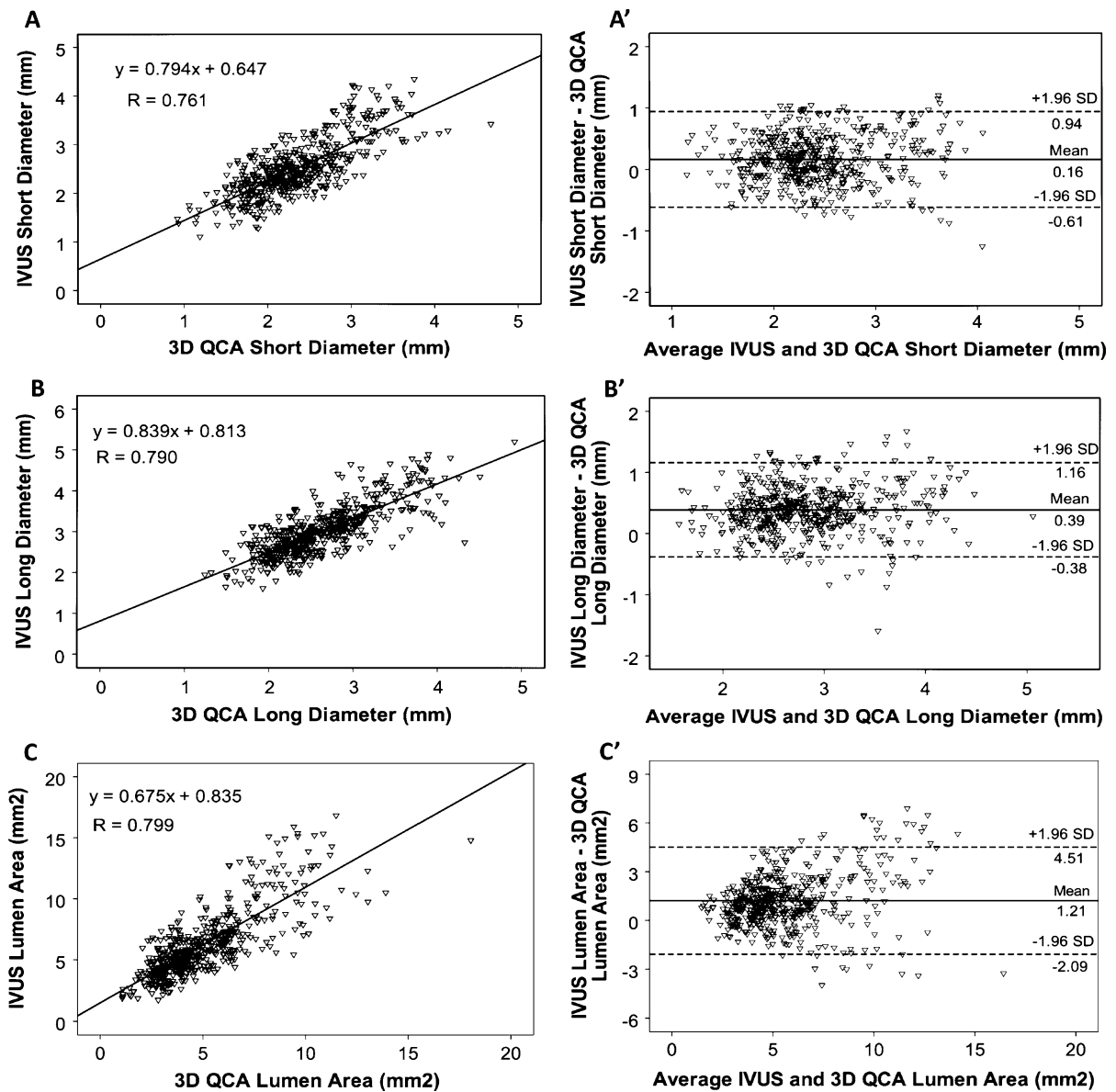
Fig. 3 Frame-based comparison between 3D QCA and IVUS. Correlations in assessing short diameter (**a**), long diameter (**b**), and area (**c**). Bland–Altman plots show the differences of the measurements in short diameter (**a′**), long diameter (**b′**), and area (**c′**). There is an increasing bias towards larger discrepancy in long diameter and area at larger vessels. $n = 519$ in 40 vessels

coronary interventions in the catheterization laboratories. It has been shown that suboptimal stent selection and deployment techniques were associated with significant risks of restenosis and thrombosis [13]. The choice of right stent size is thus important for the outcome of stenting procedures [14]. In modern catheterization laboratories, multiple imaging modalities including X-ray angiography and intracoronary imaging such as IVUS or OCT are widely available.

However, when X-ray angiography is performed in conjunction with IVUS or OCT, lumen dimensions often show discrepancies in these imaging modalities. De Scheerder [15] reported smaller lumen size as assessed by IVUS in both normal and diseased coronary arteries, while Tsuchida [16] showed that IVUS measured larger lumen size in stented vessel, as compared with QCA. The difference to some extents can be attributed to the limitations in conventional

Table 2 Comparison between 3D QCA and IVUS in assessing lumen size

	IVUS	3D QCA	Difference (95% CI)	Intra-observer variability[a]	Inter-observer variability[a]
Positions, $n = 519$					
Short diameter (mm)	2.51 ± 0.58	2.34 ± 0.56	$0.16\ (0.13–0.20)^{†}$	0.022 ± 0.131	0.025 ± 0.097
Long diameter (mm)	3.02 ± 0.62	2.63 ± 0.58	$0.39\ (0.36–0.42)^{†}$	0.039 ± 0.162	0.042 ± 0.092
Lumen area (mm^2)	6.29 ± 2.77	5.08 ± 2.34	$1.21\ (1.07–1.35)^{†}$	0.124 ± 0.534	0.134 ± 0.356
Vessels, $n = 40$					
Short diameter (mm)	2.53 ± 0.39	2.35 ± 0.37	$0.18\ (0.10–0.26)^{†}$	–	–
Long diameter (mm)	3.05 ± 0.43	2.64 ± 0.36	$0.41\ (0.34–0.48)^{†}$	–	–
Lumen area (mm^2)	6.41 ± 1.92	5.12 ± 1.45	$1.29\ (0.95–1.63)^{†}$	–	–

[a] Observer variability was calculated from 136 positions from the first 10 vessels. *CI* Confidence interval; † $P < 0.001$

QCA. To measure absolute lumen dimensions, the calibration procedure is required by conventional QCA, which can increase measurement variability and introduce the so-called out-of-plane magnification error [17]. When the vessel of interest is not aligned in the same plane as the calibration object, lumen size can be overestimated or underestimated depending on the assessed position. Another important limitation in the assumption of circular cross-sections might lead to inaccurate assessments of lumen dimensions for noncircular lesions.

To address the limitations in conventional QCA, 3D QCA was proposed and developed. By restoring vascular structures in natural shape, 3D QCA was able to resolve some of these limitations, e.g., the vessel foreshortening and out-of-plane magnification errors, and reveal more details in the arterial cross-sections. In a bench study, Tu showed that 3D QCA was able to measure lumen dimensions with high accuracy and low variability on a wide range of acquisition angles [2]. When applied in patients with coronary artery disease, 3D QCA results agreed very well with vessel segment length as compared with IVUS using motorized pullback at constant pullback speed [4] and with true balloon length [18]. In addition, 3D QCA also enabled the so-called optimal viewing angles, which could be useful to minimize foreshortening and overlap in the ostial lesions and to guide interventional procedures [3, 5]. In short, 3D QCA is on the horizon to be used more often in routine clinical practice, due to the recent developments and support of automated calibration by most modern flat-panel X-ray systems. Particularly, 3D QCA can easily be integrated with IVUS or OCT to optimize the stent sizing and positioning during the interventional

procedures [8]. While IVUS or OCT provides a wealth of information of the vessel wall, 3D QCA provides unique and complementary information including vessel tortuosity, curvature, and optimal viewing angles, et al. Such combined systems have high potential to be widely applied in routine clinical practice if a seamless workflow is implemented. It is thus desirable to understand the systematic discrepancy in order to interpret and combine different imaging modalities, especially for diffusely diseased vessels when coupled with IVUS/OCT imaging artifacts.

At present, however, limited evidence is available on the comparison between 3D QCA and IVUS or OCT. Bruining [19] evaluated 16 patients receiving a biodegradable stent and found that lumen diameter and area were smaller by IVUS than by 3D QCA. However, only vessel-based comparison was performed resulting in small sample size (11 vessels were evaluated by 3D QCA) and limited evidence. Schuurbiers [9] compared 3D QCA with IVUS on 1157 cross-sections in 10 coronary arteries using an offline co-registration tool, the ANGUS, to establish the correspondence between X-ray and IVUS images. The authors reported that 3D QCA systematically underestimated lumen area, as compared with quantitative IVUS. However, the evidence was limited by the fact that injection of diluted contrast agent during angiographic image acquisitions was required by ANGUS, which reduced the quality of the angiographic images. To our knowledge, there is no direct comparison between 3D QCA and OCT in co-registered datasets. Therefore, we developed and used a novel, real-time co-registration approach to compare 3D QCA with IVUS and OCT. Our data demonstrated that both
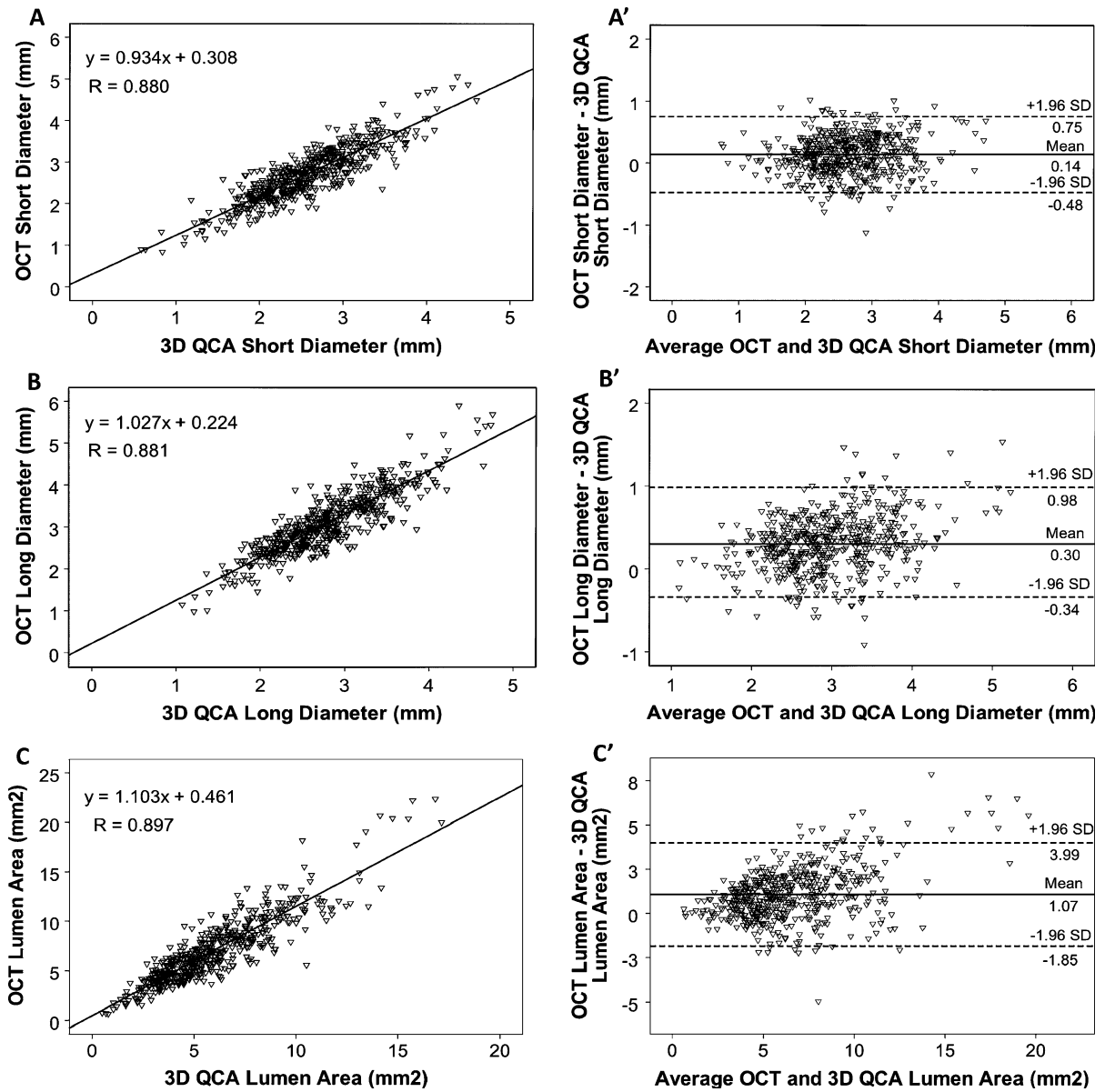
Fig. 4 Frame-based comparison between 3D QCA and OCT. Correlations in assessing short diameter (**a**), long diameter (**b**), and area (**c**). Bland–Altman plots show the differences of the measurements in short diameter (**a′**), long diameter (**b′**), and area (**c′**). There is an increasing bias towards larger discrepancy in long diameter and area at larger vessels. $n = 541$ in 40 vessels

IVUS and OCT correlated well with 3D QCA in assessing lumen size at corresponding positions. The lumen size was larger by both IVUS and OCT, however, the agreement with 3D QCA tended to be slightly better by OCT than by IVUS: The differences between OCT and 3D QCA in short diameter, long diameter, and area were 0.14 mm (5.3%), 0.30 mm (10.2%), and 1.07 mm^2 (16.5%), respectively, while

the differences between IVUS and 3D QCA were 0.16 mm (6.6%), 0.39 mm (13.8%), and 1.21 mm^2 (21.3%), respectively. These results are in line with a recent study by Okamura [20], who evaluated the optical frequency domain imaging (OFDI) in comparison to IVUS and QCA in 19 patients undergoing stent implantation. The lumen area was found the largest by IVUS, followed by OFDI, and was the smallest by

Table 3 Comparison between 3D QCA and OCT in assessing lumen size

	OCT	3D QCA	Difference (95% CI)	Intra-observer variability[a]	Inter-observer variability[a]
Positions, $n = 541$					
Short diameter (mm)	2.70 ± 0.65	2.57 ± 0.61	$0.14(0.11\text{--}0.16)^{\dagger}$	0.000 ± 0.013	0.003 ± 0.029
Long diameter (mm)	3.11 ± 0.72	2.80 ± 0.62	$0.30\ (0.27\text{--}0.33)^{\dagger}$	0.003 ± 0.024	0.006 ± 0.035
Lumen area (mm^2)	7.01 ± 3.28	5.93 ± 2.66	$1.07\ (0.95\text{--}1.20)^{\dagger}$	0.002 ± 0.039	0.021 ± 0.059
Vessels, $n = 40$					
Short diameter (mm)	2.71 ± 0.46	2.57 ± 0.43	$0.14\ (0.09\text{--}0.19)^{\dagger}$	–	–
Long diameter (mm)	3.11 ± 0.52	2.81 ± 0.45	$0.30\ (0.24\text{--}0.37)^{\dagger}$	–	–
Lumen area (mm^2)	7.02 ± 2.34	5.94 ± 1.91	$1.08\ (0.80\text{--}1.37)^{\dagger}$	–	–

[a] Observer variability was calculated from 165 positions from the first 10 vessels. *CI* Confidence interval; † $P < 0.001$
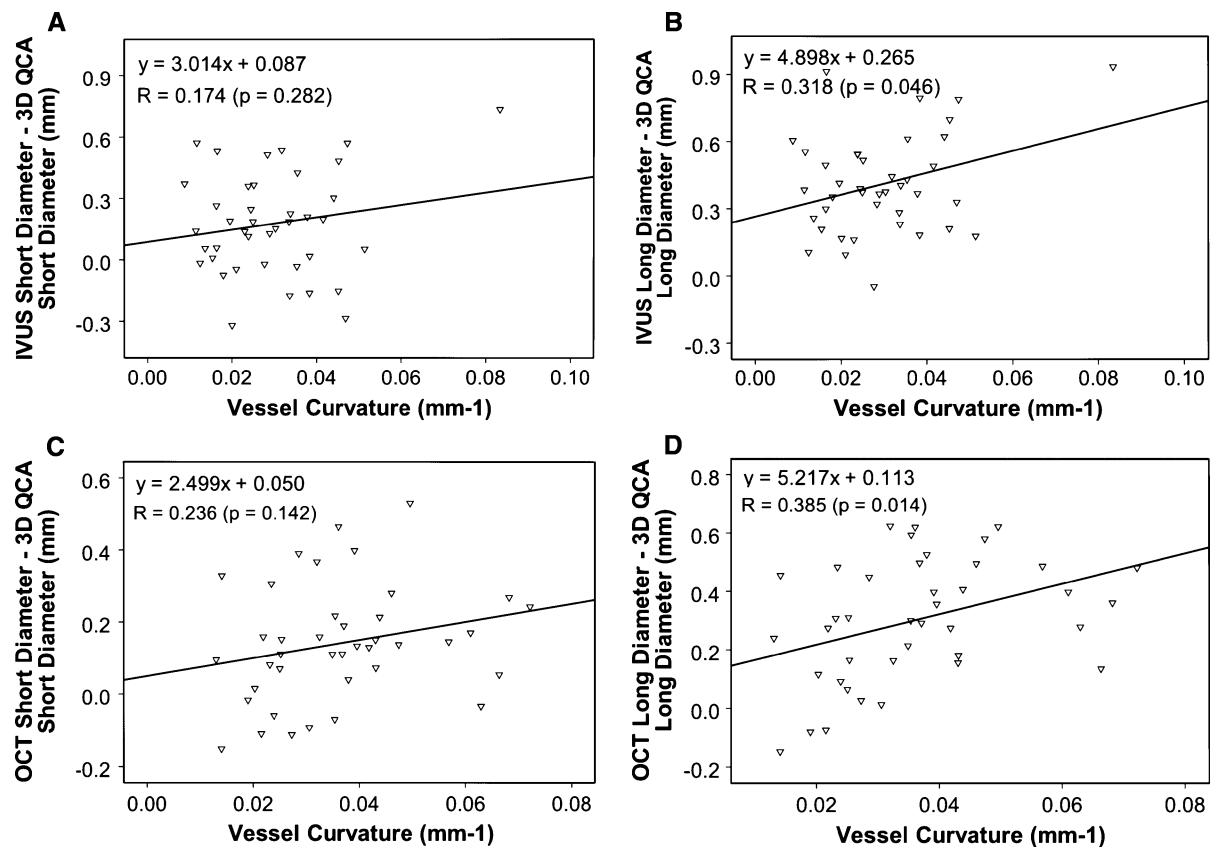
Fig. 5 Vessel-based comparison between 3D QCA and IVUS/OCT. Correlations between 3D QCA and IVUS for short diameter (**a**) and long diameter (**b**). There is an increasing bias towards larger discrepancy in long diameter at higher vessel curvature. Correlations between 3D QCA and OCT for short diameter (**c**) and long diameter (**d**). There is also an increasing bias towards larger discrepancy in long diameter at higher vessel curvature. $n = 40$ vessels in 37 patients

QCA. New in our study was that non-stented vessel segments were evaluated and 3D QCA was applied. Besides, a real-time co-registration approach was used to guarantee the point-to-point correspondence between different imaging modalities. Our results are also in agreement with previous studies by Gonzalo [1] and Suzuki [21], which showed that as compared with histology, both IVUS and OCT measured larger lumen size and the discrepancy was more pronounced by IVUS. Nevertheless, it should be

Table 4 Independent association of the discrepancy between 3D QCA and IVUS/OCT long diameter with vessel curvature and catheter looseness

	IVUS—3D QCA		OCT—3D QCA	
	β^a (95% CI)	P	β^a (95% CI)	P
Vessel curvature	5.32 (0.80–9.85)	0.02	4.63 (0.66–8.59)	0.02
Catheter looseness	0.20 (0.04–0.37)	0.02	0.14(0.10–0.26)	0.04

[a] Multiple linear regression adjusted for catheter looseness and vessel curvature. β indicates unstandardized β coefficient. *CI* Confidence interval; $n = 40$ vessels from 37 patients

borne in mind that our study does not allow a direct comparison between IVUS and OCT, since IVUS and OCT imaging were not performed in the same vessels. In addition, our study compared 3D QCA at the ED phase with OCT images which could correspond to any moment in the cardiac cycle, while 3D QCA was compared with IVUS images which were both selected at the ED phase. Last but not least, although the correspondence between different imaging modalities was established by the co-registration approach, the relatively slow pullback speed in IVUS imaging could increase local errors in the registration when coupled with patient respirations, resulting in a suboptimal match for the comparison between 3D QCA and IVUS.

Similar to the findings by Schuurbiers [9] in the comparison between 3D QCA and IVUS, our data also showed that the lumen area was larger by IVUS than by 3D QCA. However, the difference that we found by Bland–Altman plots indicated that the discrepancy was more pronounced in larger vessels, while Schuurbiers reported that the trend (lumen area was larger in IVUS) tended to reverse in larger vessels (difference lumen area $= 0.013 - 0.058 \times$ average lumen area, $P < 0.05$). The difference could be explained by the fact that suboptimal angiographic image quality using diluted contrast agent was used by Schuurbiers, while we used angiographic images with vessels well filled with contrast agent. In addition, different 3D QCA software packages and co-registration approaches were applied. Last but not least, there was no official guideline in the acquisition of angiographic images dedicated for 3D QCA in a broad clinical setting, making the interpretation of different studies difficult.

Another important finding of the present study was that vessel-based discrepancy between 3D QCA and IVUS or OCT tended to increase with the vessel curvature, especially in assessing long diameter. Tortuous vessels with high vessel curvature could lead to oblique imaging, i.e., the imaging catheter was positioned obliquely inside the lumen, and hence the circular lumen appeared elliptical in shape, resulting in overestimation of long diameter by IVUS or by OCT. This could partly explain our finding that the discrepancy between 3D QCA and IVUS or OCT was more pronounced in long diameter than in short diameter. Actually, the discrepancy in long diameter as demonstrated in this study was about two times larger than in short diameter, indicating that attention should be given when sizing the stent based on the long diameter from IVUS or OCT. An optimal stent selection should be applied from multiple assessments when combined with individual characteristics of the target vessel.

Limitations

The vessel-based comparison between different modalities was limited by the small sample size ($n = 40$). The ground truth of lumen size was not available for the comparison. In addition, 3D QCA was compared with IVUS and with OCT in different datasets and the study was limited by its retrospective in nature. For the 40 analyzed vessels from the patients undergoing IVUS imaging, intracoronary glyceryl trinitrate (GTN) was administered prior to the acquisitions of X-ray angiographic images used for 3D QCA and prior to IVUS imaging. However, for the 40 analyzed vessels from the patients undergoing OCT imaging, GTN was administrated prior to 3D QCA in 18 vessels and prior to OCT imaging in 20 vessels. GTN was not administrated or administrated after 3D

QCA and OCT imaging in 16 vessels. For the rest, the information on whether and when GTN was administrated could not be retrieved. This could create bias in comparing IVUS and OCT. Therefore, further studies using the same coronary vessels are warranted before definite conclusions about the accuracy and agreement of these three major imaging modalities in the catheterization laboratory can be drawn.

Conclusions

Our comparison of co-registered 3D QCA and invasive imaging data suggested a bias towards larger lumen dimensions by IVUS and by OCT, which was more pronounced in larger and tortuous vessels.

Conflict of interest Shengxian Tu and Gerhard Koning are employed by Medis medical imaging systems bv and have a research appointment at the Leiden University Medical Center (LUMC). Jurgen Ligthart has a proctor contract with Boston Scientific and provides training services for Volcano Inc and St. Jude medical. He is also a consultant of his own company LIMIC Medical. Johan H. C. Reiber is the CEO of Medis medical imaging systems bv, and has a part-time appointment at LUMC as Prof of Medical Imaging.

References

1. Gonzalo N, Serruys PW, García-García HM et al (2009) Quantitative ex vivo and in vivo comparison of lumen dimensions measured by optical coherence tomography and intravascular ultrasound in human coronary arteries. Rev Esp Cardiol 62:615–624
2. Tu S, Holm N, Koning G, Maeng M, Reiber JHC (2011) The impact of acquisition angle difference on three-dimensional quantitative coronary angiography. Catheter Cardiovasc Interv 78:214–222
3. Tu S, Jing J, Holm NR, Onsea K, Zhang T, Adriaenssens T, Dubois C, Desmet W, Thuesen L, Chen Y, Reiber JHC (2011) In vivo Assessment of bifurcation optimal viewing angles and bifurcation angles by three-dimensional (3D) quantitative coronary angiography. Int J Cardiovasc imaging. Epub Ahead of Print. doi: 10.1007/s10554-011-9996-x
4. Tu S, Huang Z, Koning G, Cui K, Reiber JHC (2010) A novel three-dimensional quantitative coronary angiography system: in vivo comparison with intravascular ultrasound for assessing arterial segment length. Catheter Cardiovasc Interv 76:291–298
5. Tu S, Hao P, Koning G et al (2011) In vivo assessment of optimal viewing angles from X-ray coronary angiograms. EuroIntervention 7:112–120
6. Reiber JHC, Serruys PW, Kooijman CJ et al (1985) Assessment of short-, medium-, and long-term variations in arterial dimensions from computer-assisted quantitation of coronary cineangiograms. Circulation 71:280–288
7. Tuinenburg JC, Koning G, Rareş A, Janssen JP, Lansky AJ, Reiber JHC (2011) Dedicated bifurcation analysis: basic principles. Int J Cardiovasc Imaging 27:167–174
8. Tu S, Holm NR, Koning G, Huang Z, Reiber JHC (2011) Fusion of 3D QCA and IVUS/OCT. Int J Cardiovasc Imaging 27:197–207
9. Schuurbiers JC, Lopez NG, Ligthart J et al (2009) In vivo validation of CAAS QCA-3D coronary reconstruction using fusion of angiography and intravascular ultrasound (ANGUS). Catheter Cardiovasc Interv 73:620–626
10. Wahle A, Lopez JJ, Olszewski ME et al (2006) Plaque development, vessel curvature, and wall shear stress in coronary arteries assessed by X-ray angiography and intravascular ultrasound. Med Image Anal 10:615–631
11. Koning G, Dijkstra J, von Birgelen C et al (2002) Advanced contour detection for three-dimensional intracoronary ultrasound: a validation—in vitro and in vivo. Int J Cardiovasc Imaging 18:235–248
12. Tu S, Koning G, Tuinenburg JC et al (2009) Coronary angiography enhancement for visualization. Int J Cardiovasc Imaging 25:657–667
13. Costa MA, Angiolillo DJ, Tannenbaum M et al (2008) Impact of stent deployment procedural factors on long-term effectiveness and safety of sirolimus-eluting stents (final results of the multicenter prospective STLLR trial). Am J Cardiol 101:1704–1711
14. Gollapudi RR, Valencia R, Lee SS et al (2007) Utility of three-dimensional reconstruction of coronary angiography to guide percutaneous coronary intervention. Catheter Cardiovasc Interv 69:479–482
15. De Scheerder I, De Man F, Herregods MC et al (1994) Intravascular ultrasound versus angiography for measurement of luminal diameters in normal and diseased coronary arteries. Am Heart J 127:243–251
16. Tsuchida K, Serruys PW, Bruining N et al (2007) Two-year serial coronary angiographic and intravascular ultrasound analysis of in-stent angiographic late lumen loss and ultrasonic neointimal volume from the TAXUS II trial. Am J Cardiol 99:607–615
17. Koning G, Hekking E, Kemppainen JS et al (2001) Suitability of the Cordis Stabilizer™ marker guide wire for quantitative coronary angiography calibration: an in vitro and in vivo study. Catheter Cardiovasc Interv 52:334–341
18. Rittger H, Schertel B, Schmidt M et al (2009) Three-dimensional reconstruction allows accurate quantification and length measurements of coronary artery stenoses. EuroIntervention 5:127–132
19. Bruining N, Tanimoto S, Otsuka M et al (2008) Quantitative multi-modality imaging analysis of a bioabsorbable poly-L-lactid acid stent design in the acute phase: a comparison between 2 and 3D-QCA, QCU and QMSCT-CA. EuroIntervention 4:285–291

20. Okamura T, Onuma Y, Garcia–Garcia HM et al (2011) First-in-man evaluation of intravascular optical frequency domain imaging (OFDI) of Terumo: a comparison with intravascular ultrasound and quantitative coronary angiography. EuroIntervention 6:1037–1045

21. Suzuki Y, Ikeno F, Koizumi T et al (2008) In vivo comparison between optical coherence tomography and intravascular ultrasound for detecting small degrees of in-stent neointima after stent implantation. JACC Cardiovasc Interv 1:168–173